Proceeding of the IEEE
International Conference on Robotics and Biomimetics
Dali, China, December 2019

A Highly Mobile Crawling Robot Inspired by Hexapod Insects*

Mingyuan Yang, Rongjie Kang and Yan Chen
Key Laboratory of Mechanism Theory and Equipment Design of the Ministry of Education
School of Mechanical Engineering, Tianjin University
Tianjin Province, China
yan_chen@tju.edu.cn

***Abstract* - Rescue robots are usually used in security and disaster investigating missions. Yet the complex control and actuation systems make them very heavy and expensive. This paper proposed a novel crawling robot named "HIbot" inspired by hexapod insect with low cost, light weight and simple control. Both movable body and legged-wheel were adapted to achieve fixable movement of the robots with one DC motor and no extra control. A series of experiments demonstrated that the HIbot can crawl in various outdoor environments such as gravel, grassland, etc. It can cross obstacles that are as high as 2.8 times of the radius of the legged-wheel. Such characteristics give the robot a great potential in applications.**

Index Terms – Rescue robots. Crawling robot. Legged-wheel. Bio-inspired robots. Mechanical intelligence.

I. INTRODUCTION

In large-scale disaster sites, such as earthquakes, landslides, hurricanes and so on, the number of professional rescuers cannot meet the demand [1]. Furthermore, disaster sites are full of collapsed structures, which makes it difficult to access. Therefore, the development of disaster rescue robots bears great significance.

Bio-inspired robots have attracted increasing attention in recent years. Snake robots are a typical kind of rescue bio-robots [1]-[6]. They are suitable to explore narrow space because of their smart bodies and multiple freedoms. Particular interest has been drawn to the insects, who have small brain but exhibit amazing embodiment intelligence through the interactions between their bodies and surrounding environments [7]. For instance, their bodies and legs can adapt to various rough terrains and generate fast movements without participation of central nerve systems. How to transfer such embodiment intelligence found on insects to sort of mechanical intelligence for crawling robots to achieve efficient locomotion with simple structure and control system is the challenge of this paper.

Through the observation of the movements of insects such as mantis and ants, we found that they have a movable multi-segmented body. When encountering an vertical obstacle, they will lift the front segment of the body to increase its ability to climb obstacles [8]. Hence, some rescue robots use tracks and a movable body to move in the ruins [9]-[12]. Their bodies are divided into many segments. Through the interaction between the body segments, such robots can climb over large obstacles.

Crawling robots such as RHex [13], ASGUARD [14], Wheg I [15], Wheg II [16] and DAGSI WhegsTM [17] have four or six legged-wheels which can walk in complex outdoor terrains. Most of them were inspired by insects. The key idea is to use a motor to drive one or more simple legs on a rotating wheel. Legged-wheels have the advantages of both the legs and wheels. The simple, but very robust, hybrid legged-wheeled robot have good application potential in disaster rescue. ASGUARD [14] and Wheg I [15] used the whegs (i.e. legged-wheels) with equal angles. According to Roger D. Quinn's [15] description, a two-spoke wheg with equal angles would have better climbing abilities, but difficult to walk. A four-spoke wheg with equal angles would be less capable for climbing steps, but would provide a smoother ride. The three-spoke wheg with equal angles makes a trade-off between the climbing ability and the ride smoothness. They can move quickly and climb over large obstacles.

Therefore, in this paper, the robot called HIbot with two body segments and six whegs is specifically built for climbing obstacles in disaster sites, aiming to achieve light weight, low cost while maintaining high mobility and reliability. The paper is organized as follows. Section II introduces the construction of our robotic system. Sections III and IV describes the analysis of the legged-wheels and the movable body, respectively. Section V presents the results of experiments. The concludes this study is drawn in Section VI.

II. SYSTEM DESCRIPTION

A. General construction of the HIbot

The presented hexapod robot, depicted in Fig. 1, is comprised of two body segments. The front body segment is 220mm long, 100mm wide and 85mm high. The rear body segment has the same length and height, but is 110mm in width. The two segments are connected with a free joint allowing the robot to passively lift the front segment when encountering obstacles. Six four-spoke whegs are installed on both sides of the body. The radius of the wheg (i.e. the length of the leg) is 75mm. To achieve the lightweight design, only one drive motor is located on the rear body segment. Motor power is transmitted to three drive axles via a one-level speed reducer and synchronous belt drive system. The material of the

* Financial support from the Natural Science Foundation of China (Projects No. 51825503 and No. 51721003).

978-1-7281-6321-5/19//$31.00 ©2019 IEEE

body is acrylonitrile butadiene styrene plastic (i.e. ABS). The total weight of the HIbot is about 440g. There is no control element in the robot. We only use an on/off switch connected to the power source (battery here).

B. *Four-spoke Whegs*

Whegs have the advantages of both the legs and wheels. They can move quickly and climb over large obstacles. The HIbot have six four-spoke whegs with unequal angles. The phase difference of whegs 1, 2 and whegs 2, 3 are both 30 degrees, which make the robot have a strong climbing ability while walking smoothly. The detailed description of whegs will be introduced in Section III.

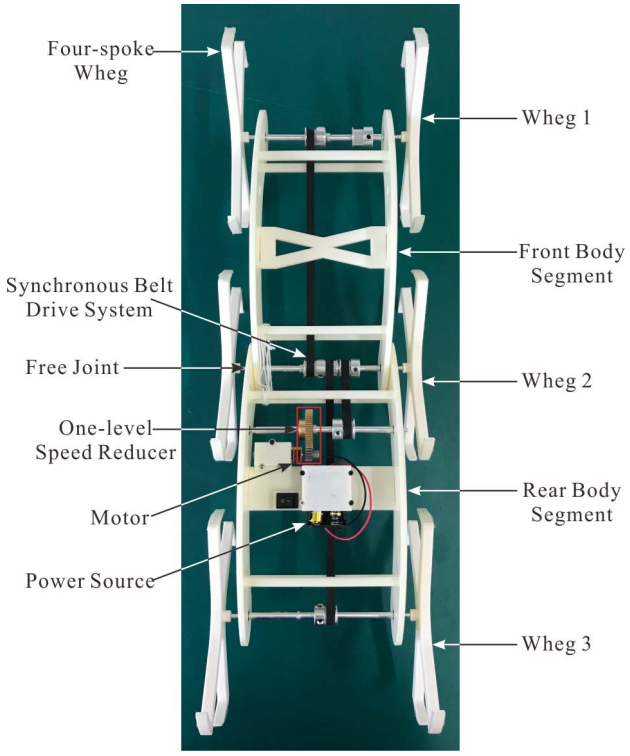

Fig. 1 Main components of the HIbot.

C. *Actuation*

Most crawling robots are driven by many actuators. For instance, the RHex robot designed by Boston Dynamics uses six motors to control the legs, which results in a significant increase in the weight and computation cost of the robot. To solve this problem, the HIbot uses a single DC motor to propel itself. The motor power is transmitted to three drive axles of the whegs via a one-level speed reducer and synchronous belt drive system (Fig. 1). The weight of the single-motor robot is much less than the robots with legs or joints driven by individual motors.

III. Design of the Whegs

Comparing the advantanges and disadvantages of three-spoke wheg and four-spoke wheg, we propose a four-spoke wheg with unequal angles.

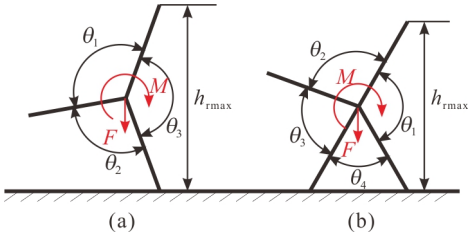

Fig. 2 Multi-spoke whegs with unequal angles. (a) Three-spoke wheg with unequal angles. (b) Four-spoke wheg with unequal angles.

Actually, the angles of the wheg are not necessarily equal. Different performance can be obtained by changing the angles of the wheg. As shown in Fig. 2, $h_{r\max}$ is the maximum height that the leg can reach. $M_{\max}$ is the maximum driving force that the motor needs to provide. If the force that the body acting on the center of the wheg, F, is constant, we can obtain the equations of $h_{r\max}$ and $M_{\max}$.

$$h_{r\max} = 2r\sin\frac{\theta_{\max}}{2}, \tag{1}$$

$$M_{\max} = Fr\sin\frac{\theta_{\max}}{2}. \tag{2}$$

In (1) and (2), r is the length of the leg. $\theta_{\max}$ is the maximum of $\theta_1,\theta_2,\theta_3,\theta_4$. From (1) and (2), we can know that $h_{r\max}$ and $M_{\max}$ are proportional to $\theta_{\max}$. If we neither increase the motor load nor reduce the climbing ability, $\theta_{\max}$ can only be $120°$. For three-spoke whegs, the configuration that satisfies $\theta_{\max}=120°$ is only $\theta_1=\theta_2=\theta_3=120°$ (i.e. three-spoke wheg with equal angles). For four-spoke whegs, there are many configurations that satisfy $\theta_{\max}=120°$. Figure 3 shows three configurations for four-spoke whegs where $\theta_{\max}=120°$. These three whegs are the improved design for three-spoke wheg with equal angles, so we use the analysis of the three-spoke wheg as an example to introduce the performance of these whegs.

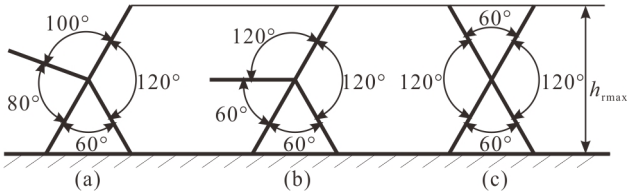

Fig. 3 Four-spoke whegs with unequal angles. (a) Four-spoke Wheg I. (b) Four-spoke Wheg II. (c) Four-spoke Wheg III.

We first analyzed the impact of wheg phase on robot climbing ability. As shown in Fig. 4, θ_2 is the angle between the supporting leg of wheg 2 and the vertical direction. $L_{12}=180$ mm is the wheelbase between whegs 1 and 2. γ is the angle between the front body segment and the horizontal

ground. $\gamma_{max}=60°$ is the maximum of γ, which is determined by the body structure. θ_{12} is the phase difference of wheg 2 relative to wheg 1. θ_{23} is the phase difference of wheg 3 relative to wheg 2. h_{max} is the maximum height that the leg of wheg 1 can reach.

$$h_{max}=r_2\cos\theta_2+r_1\sin 60°+L_{12}\sin\gamma_{max}, \quad (3)$$

$$\theta_2=\theta_{12}-30°, \quad \theta_{12}\in[0,60°]. \quad (4)$$

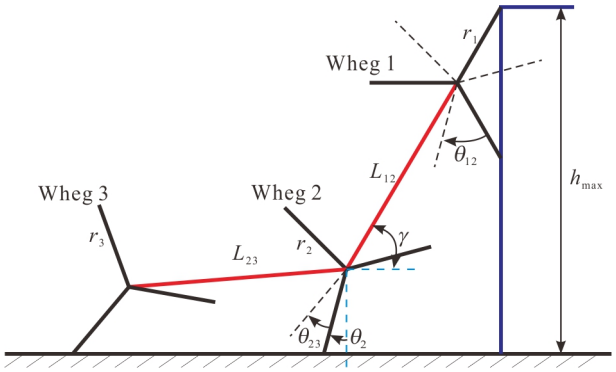

Fig. 4 Schematic of the HIbot with three-spoke whegs.

Because we have limited the value of γ_{max}, h_{max} has no relationship with θ_{23}. The relationship between h_{max} and θ_{12} is shown in Fig. 5. It can be seen that, the leg of wheg 1 can reach the largest climbing height h_{max} =295.84mm when $\theta_{12}=30°$. By using the same method, we analyzed the other three whegs and got the following conclusions. For Four-spoke Wheg I, II and III, when $\theta_{12}=30°$, the leg of front whegs can all reach the largest climbing height. The largest climbing height for these three whegs are all 295.84mm.

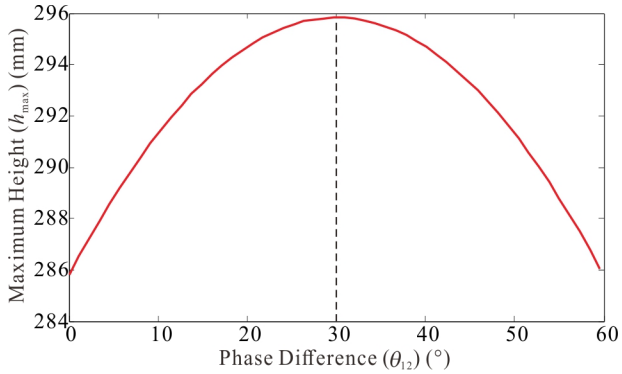

Fig. 5 The relationship curve between the maximum height and the phase difference.

We also analyze the impact of wheg phase on the smoothness of robot motion. As shown in Fig. 6, the robot walks in the direction shown by the arrow. We ignore the curved claws at the end of the legs and treat the legs as three equal line segments that intersect at one point. The angles between the line segments are both 120 degrees. The whegs are defined as whegs 1, 2, 3 and rotate in a clockwise direction. The radius of the whegs are r_1, r_2, r_3, respectively. The legs of each wheg are defined as legs 1, 2, and 3. θ is the angle that leg 1 of wheg 1 rotates clockwise from the vertical state. In Fig. 6, $\theta=300°$ (i.e. $\theta=-60°$). O_{12}, O_{23} are the center positions of the front and rear body segments, respectively. Only the change in the height of the front body segment center during movement is now analyzed. The same method can be applied to the analysis of the rear body segment.

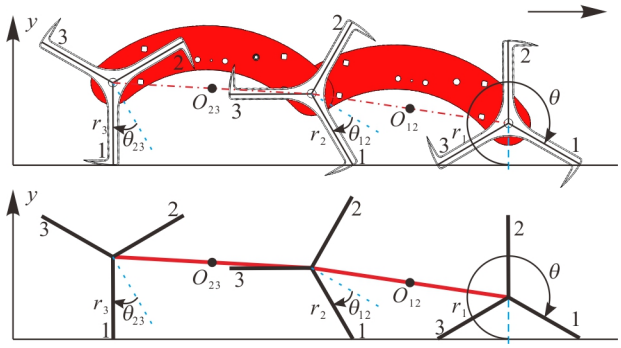

Fig. 6 Schematic of the HIbot with three-spoke whegs.

$$y_{O12}=0.5(y_1+y_2), \quad (5)$$

$$\Delta y_{O12max}=y_{O12max}-y_{O12min}, \quad (6)$$

$$y_1=\begin{cases} r_1\cos\theta, & \theta\in[-60°,60°) \\ r_1\cos(\frac{2\pi}{3}-\theta), & \theta\in[60°,180°) \\ r_1\cos(\frac{4\pi}{3}-\theta), & \theta\in[180°,300°] \end{cases}, \quad (7)$$

$$y_2=\begin{cases} r_2\cos(\theta+\theta_{12}), & \theta\in[-60°,60°-\theta_{12}) \\ r_2\cos(\frac{2\pi}{3}-\theta-\theta_{12}), & \theta\in[60°-\theta_{12},180°-\theta_{12}) \\ r_2\cos(\frac{4\pi}{3}-\theta-\theta_{12}), & \theta\in[180°-\theta_{12},300°-\theta_{12}) \\ r_2\cos(2\pi-\theta-\theta_{12}), & \theta\in[300°-\theta_{12},300°] \end{cases}, \quad (8)$$

where y_1, y_2 are the heights of the centers of whegs 1 and 2 respectively. y_{O12} is the height of the front body center. y_{O12max} is the maximum height of the body center during the movement. y_{O12min} is the minimum height of the body center during the movement. Δy_{O12max} is the maximum change in the height of the body center. $r_1=r_2$=75mm, $\theta_{12}\in[0°,120°)$. By

changing the value of θ_{12}, a relationship between $\Delta y_{O12\max}$ and θ_{12} can be obtained.

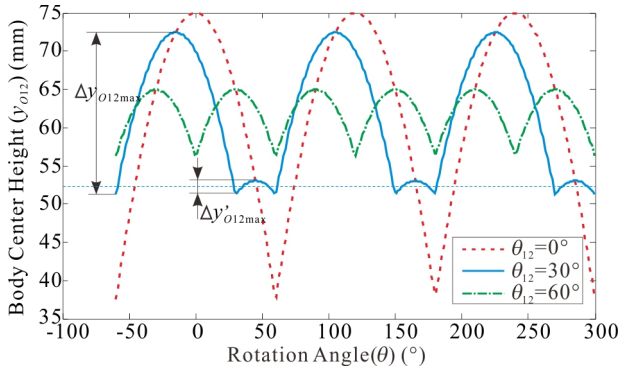

Fig. 7 The relationship between the height of the body center and the rotation angle of the three-spoke wheg under different phase.

As shown in Fig. 7, although $\Delta y_{O12\max}$ has the maximum when $\theta_{12}=0°$, the body center has only three large changes during one rotation of the wheg. Compared with the case of $\theta_{12}=60°$, although $\Delta y_{O12\max}$ has the minimum when $\theta_{12}=60°$, the body center has six large changes during one rotation of the wheg. Compared with large amplitude and low frequency vibrations, small amplitude and high frequency ones may cause more damage to the robot. The configuration of $\theta_{12}=30°$ can be seen as the compromise between $\theta_{12}=0°$ and $\theta_{12}=60°$.

By using the same analysis method, we get the relationship between the height of the body center and the rotation angle of these three whegs where $\theta_{12}=30°$. As shown in Fig. 8, the Four-spoke Wheg III have smoother ride than the Four-spoke Whegs I and II. So we choose the Four-spoke Wheg III as the wheg of the HIbot.

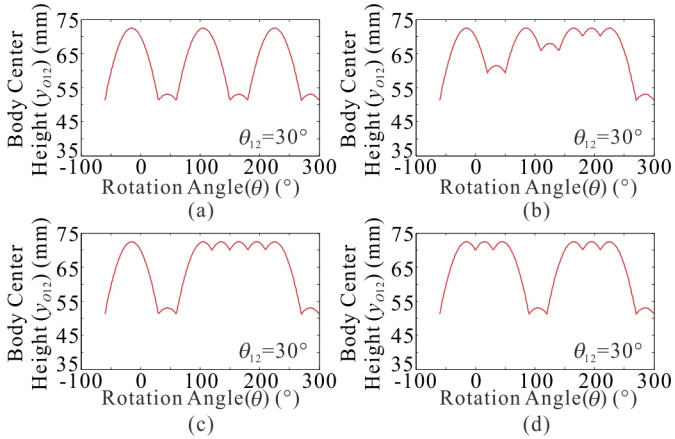

Fig. 8 Center height of the front segment when the robot moves horizontally in different phases. (a) Three-spoke wheg. (b) Four-spoke Wheg I. (c) Four-spoke Wheg II. (d) Four-spoke Wheg III.

IV. Simulation Analysis of the Movable Body

The HIbot is comprised of two body segments, which are connected with a free joint, the length of the two segments is equal. The purpose of the free joint is to increase the adaptability of the robot to the ground environment.

We used SolidWorks Motion to simulate the motion of the robot on ditches. The simulation environment is a ground surface with uniformly distributed ditches. The width of the ditch is 160mm, which is slightly larger than the diameter of the four-spoke wheg. The depth of the ditch is 75mm, which is equal to the radius of the wheg. The space between adjacent ditches is 200mm, which is slightly larger than the wheelbase of the single segment. The static friction factor between the rim and the ground is 0.4.

Two types of robots were used for simulation analysis. Type 1 has a fixed joint so that the two body segments cannot rotate freely around the joint. Type 2 uses a free joint and the two body segments can rotate about the joint freely. All the other structures, parameters and materials of the two robots are the same as described in Section IIA. The wheg speed follows the 3-4-5 polynomial motion at 0~1s, because the speed and acceleration curves of this motion are continuous at the beginning and the end, thus no rigid and flexible impact. The speed is 0 at 0s and 20 rpm at 1s, and then following a constant speed. The simulation time is set to 20s. The simulation results of the two robots on the ditch ground are shown in Fig. 9 and 10. It can be found from Fig.9 that Type1 has the front wheg floating during the motion at 4s, 6s, 14s and 20s. When the front wheel touching the ground, it will bring an impact that may cause damages to the robot. Since the two body segments of Type 2 can rotate about the free joint passively, the three sets of whegs are always in contact with the ground during the whole movement. Therefore, Type 2 has better ground environment adaptability.

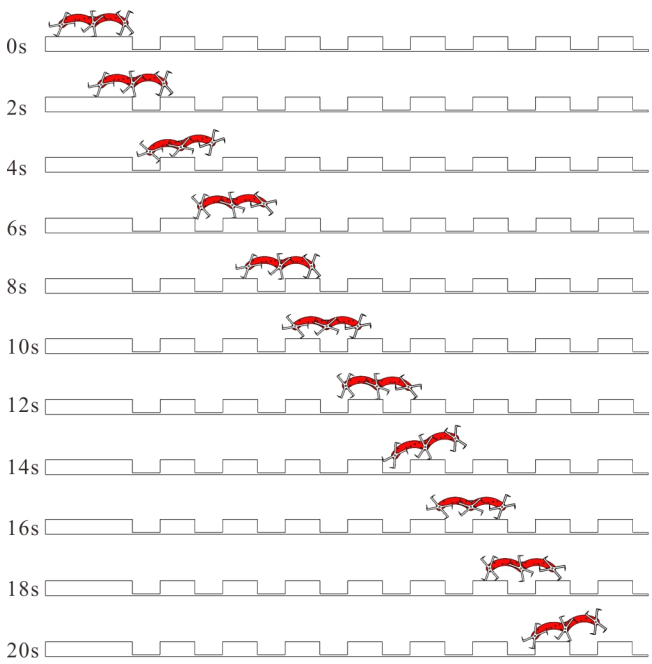

Fig. 9 Simulation diagram of climbing gait (ditch ground, fixed joint)

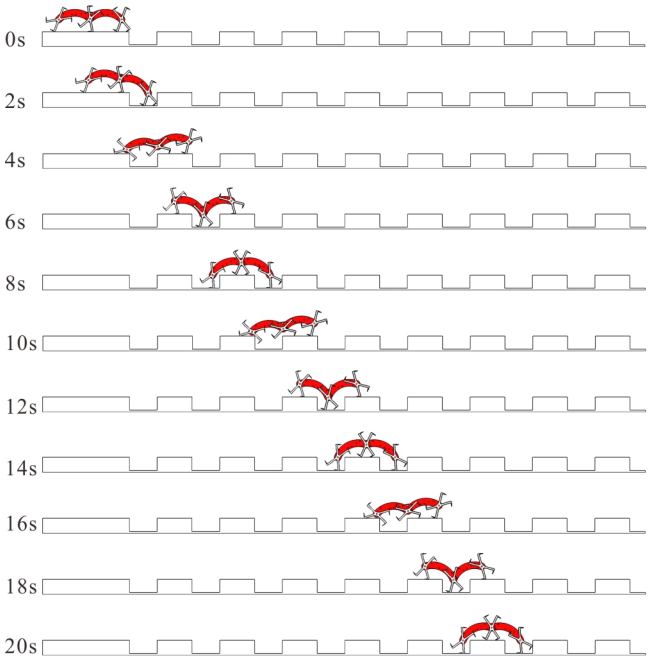

Fig. 10 Simulation diagram of climbing gait (ditch ground, free joint)

V. Experiments

The performance of the HIbot was tested in different conditions. It can walk in a variety of outdoor environments such as gravel and grassland (Fig. 11). It can also climb stairs (Fig. 12).

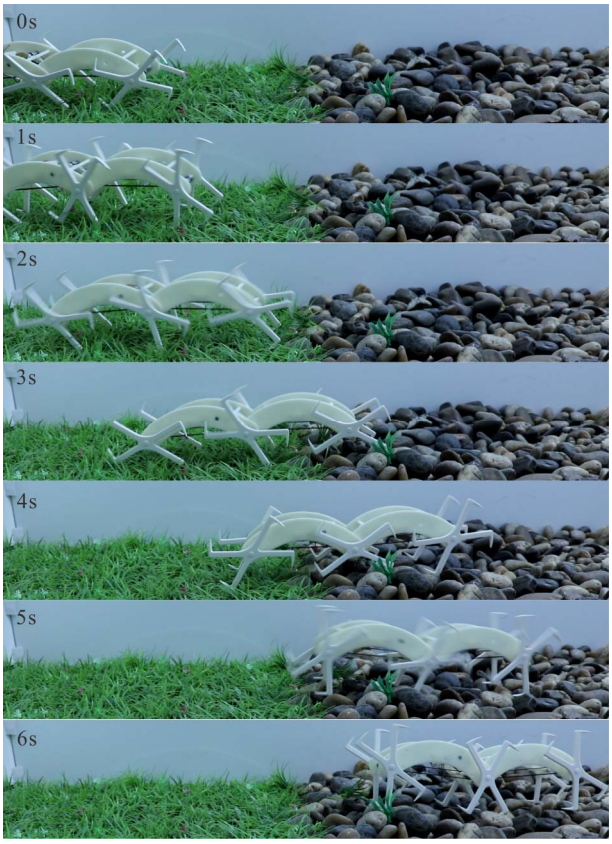

Fig. 11 HIbot walks on grassland and gravel.

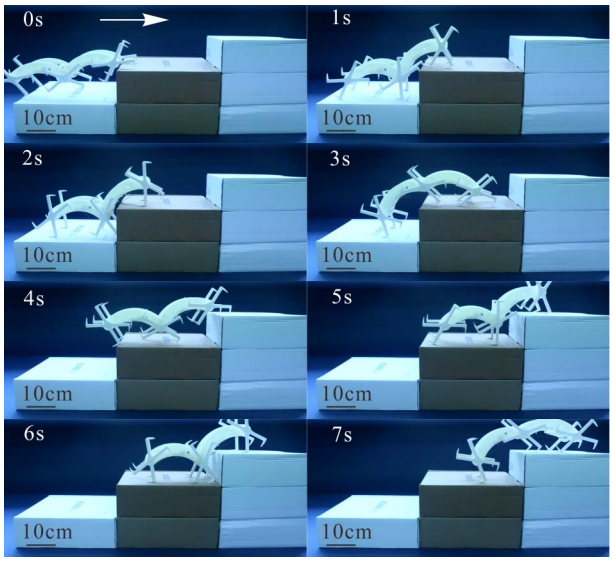

Fig. 12 HIbot climbs stairs. The height of each step is 1.4 times the radius of the wheg.

We tested the climbing ability of the HIbot. As shown in Fig. 13, HIbot can climb obstacles as tall as 2.8 times the radius of the wheg without any active control. The obstacle in Fig. 13 consists of two identical boxes, each of which is 105 mm in height.

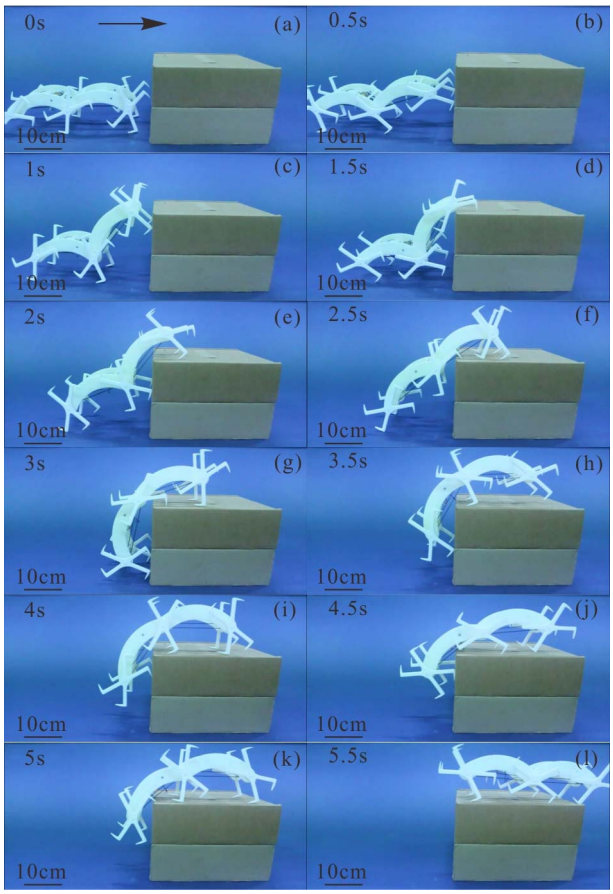

Fig. 13 HIbot climbs an obstacle as tall as 2.8 times the radius of the wheg.

When the front whegs of the HIbot encounter the obstacle, the friction between the front wheg and obstacle will lift the front body segment, as shown in Fig. 13(b) and (c).

After the end of the front whegs were hooked on the edge of the obstacle, the front whegs will climb up the obstacle easily (Fig. 13(d)). It is similar to the way that ants use the end hooks of their legs to drag the body to climb obstacles.

When the middle whegs encounter the obstacle, they will also climb along the obstacle like the front whegs (Fig. 13(e)). Once the end of the middle whegs were hooked on the edge of the obstacle, the middle whegs will also climb up the obstacle easily, as shown in Fig. 13(f) and (g).

The rear whegs climb obstacle in the same way as the front and middle whegs.

VI. Conclusion

Inspired by the movements of hexapod insects, we developed a highly mobile crawling robot using its body and leg mechanisms to adapt to environments. The body of the HIbot is formed by two segments connected with a free joint. When HIbot encounters an obstacle during locomotion, it will lift the front segment passively due to the friction between the whegs and the obstacle. Four types of the whegs have been analyzed. The results show that although the four types of the whegs have the same largest climbing height, Four-spoke Wheg III has smoother ride than three-spoke wheg, Four-spoke Wheg I and II. Experimental results show that the HIbot has high motion ability even under rough terrains. It can climb obstacles as tall as 2.8 times the radius of the wheg without any control.

HIbot has good ground environment adaptability, but it also needs the steering capability to adapt to complex environment of the disaster site. Future work will introduce a steering mechanism into the robot. Because the presented robotic prototype is to verify the motion performance and environmental adaptability, the low-speed and high-torque DC fixed-speed motor is selected. HIbot moves at a speed of 0.225m/s. In the future, high-torque DC servomotor can be used to adjust the speed to further enhance the performance of the robot.

This work shows the possibility of achieving low level robust motion control by appropriate combination of mechanical components requiring no additional computation on an electronic controller, which reduces the system complexity, as well as the weight and cost. This characteristic can be referred to as mechanical intelligence [1], [18]. Future work will further take inspirations from the body-environment interplayed behaviors of animals, and investigate cooperation strategies between mechanical and computational intelligence in a robotic system.

References

[1] Z. Yang, K. Ito, K. Hirotsune, K. Saijo, A. Gofuku, and F. Matsuno, “A mechanical intelligence in assisting the navigation by a force feedback steering wheel for a snake rescue robot,” in *Proc. IEEE Int. Workshop Robot Human Interact. Commun.*, Kurashiki, Japan, Sep. 2004, pp. 113–118.

[2] S**.** Hirose, *Biologically Inspired Robots: Snake-Like Locomotors and Manipulators*, Oxford University Press, 1993.

[3] M. Yamakita, M. Hashimoto and T. Yamada, “Control of Locomotion and Head Configuration of 3D Snake Robot”, in *Proceedings of the 2003 IEEE International Conference on Robotics and Automation*, pp. 2055-2060, 2003.

[4] S. Hirose and M. Mori, “Biologically inspired snake-like robots,” in *Proc. ROBIO 2004. IEEE Int. Conf. Robot. Biomimetics,* 2004, pp. 1–7.

[5] A. Crespi and A. J. Ijspeert, “Amphibot ii: An amphibious snake robot that crawls and swims using a central pattern generator,” in *Proc. 9th Int. Conf. Climbing Walking Robots*, no. BIOROB-CONF-2006-001, 2006, pp. 19–27.

[6] M. Luo *et al.*, “OriSnake: Design, Fabrication, and Experimental Analysis of a 3-D Origami Snake Robot,” *IEEE Robotics and Automation Letters*, 2018, vol. 3(3), pp. 1993-1999.

[7] R. Pfeifer, M. Lungarella, F. Iida. “Self-Organization, Embodiment, and Biologically Inspired Robotics,” *Science*, 2007, vol. 318(5853), pp. 1088-1093.

[8] A. Lozano, G. Peters, D. K. Liu. “Analysis of an arthropodal system for design of a climbing robot,” in *Proceedings of the 28th International Symposium of Automation and Robotics in Construction*, pp. 832-838, 2011.

[9] C. Zong, Z. Ji, Z. Chen. “A joint double-tracked robot with passive track adjusting device,” in *2018 Chinese Control and Decision Conference (CCDC). IEEE*, 2018, pp. 4148-4153.

[10] K. Nagatani *et al.*, “Redesign of rescue mobile robot Quince,” in *Proc. IEEE Int. Symp. Safety, Security, and Rescue Robotics*, pp. 13–18, 2011.

[11] M. J. Micire, “Evolution and field performance of a rescue robot,” *Journal of Field Robotics*, vol. 25(1□2), pp. 17-30, 2008.

[12] A. Birk, K. Pathak, S. Schwertfeger, and W. Chonnaparamutt, “The IUB Rugbot: an intelligent, rugged mobile robot for search and rescue operations,” in *IEEE International Workshop on Safety, Security, and Rescue Robotics (SSRR)*. IEEE Press, 2006.

[13] U. Saranli, M. Buehler, and D. Koditschek, "Rhex: A simple and highly mobile hexapod robot," *The International Journal of Robotics Research*, vol. 20, no. 7, pp. 616-63 1, July 2001.

[14] M. Eich, F Grimminger, S. Bosse, D. Spenneberg, and F. Kirchner, "Asguard: A hybrid legged wheel security and sar-robot using bio-inspired locomotion for rough terrain," in *IARP/EURON Workshop on Robotics for Risky Interventions and Environmental Surveillance*, Benicssim, Spain, January 7-8 2008.

[15] J. Quinn, R. D., Offi, D. Kingsley, and R. Ritzmann, "Improved mobility through abstracted biological principles," in *IEEE/RSJ International Conference on Intelligent Robots and System*, vol. 3, 2002, pp. 2652-2657.

[16] T. Allen, R. Quinn, R. Bachmann, and R. Ritzmann, "Abstracted biologi- cal principles applied with reduced actuation improve mobility of legged vehicles," in *Proceedings. 2003 IEEE/RSJ International Conference on Intelligent Robots and Systems (IROS2003)*, vol. 2, 2003, pp. 1370-1375.

[17] A. S. Boxerbaum, J. Oro, G. Peterson, and R. Quinn, “The latest generation whegs robot features a passive-compliant body joint,” *International Conference on Intelligent Robots and Systems*, September 2008.

[18] P. S. Sreetharan, “Mechanical Intelligence in Millimeter-Scale Machines,” Ph.D. dissertation, Harvard Univ., Cambridge, MA, 2012.